ISSN 1063-7850, Technical Physics Letters, 2012, Vol. 38, No. 5, pp. 405–408. © Pleiades Publishing, Ltd., 2012.
Original Russian Text © A.O. Podolian, A.B. Nadtochiy, O.A. Korotchenkov, 2012, published in Pis'ma v Zhurnal Tekhnicheskoi Fiziki, 2012, Vol. 38, No. 9, pp. 15–22.

Charge Carrier Lifetime Recovery in γ-Irradiated Silicon under the Action of Ultrasound

A. O. Podolian*, A. B. Nadtochiy, and O. A. Korotchenkov

Taras Shevchenko National University of Kyiv, 01601 Kyiv, Ukraine

**e-mail: gogi@univ.kiev.ua*

Received October 31, 2011

Abstract—Ultrasonic treatment of γ-irradiated silicon can lead to a significant (up to about 70%) recovery of the minority carrier lifetime reduced by the irradiation. A mechanism of the ultrasound-induced recovery is proposed, which is based on the release of vacancies from E-type centers followed by their trapping on defect sinks. It is suggested that the role of defect sinks can be played by A-type microdefects.

DOI: 10.1134/S1063785012050124

Radiation-induced defects in silicon have been extensively studied in recent decades because Si-detectors are finding increasing use both in experimental high-energy physics and in a broad spectrum of industrial, medical, spacecraft, and military devices [1–3]. In particular, these investigations have been stimulated by wide application of Si microstrip and Si pixel detectors for precision tracking of charged particles in experiments on the Large Hadron Collider at CERN [4].

Si-detectors are in most cases manufactured from high-ohmic ($\rho = 1$–6 kΩ cm) phosphorus-doped *n*-type material grown by the float-zone (FZ) technique[3, 5]. Owing to the high resistivity of FZ-Si, the depletion regime in Si-detectors is attained at relatively low working voltages. In contrast, the resistivity of single-crystalline silicon grown by the Czochralski (Cz) technique is much lower and, hence, working voltages corresponding to the full-depletion regime are high so that they exceed the breakdown threshold, which hinders the application of bias that would ensure the effective collection of charge carriers. It should be noted, however, that the Cz-Si growth techniques are continuously developed so as to provide radiation-resistant material for Si-detectors [6].

A general problem in the use of radiation detectors is related to the degradation of their characteristics under irradiation, in particular, a decrease in the minority carrier lifetime. Heat treatment of irradiated silicon, which can significantly suppress the undesired radiation-induced defects is a traditional method for recovery of the working characteristics of Si-detectors [7, 8]. However, a high-temperature annealing favors the generation of thermo-induced defects that also negatively influence the working characteristics of Si-detectors.

A promising solution to this problem is offered by the ultrasound treatment (UST) of irradiated silicon, which can reduce the concentration of radiation defects at a moderate heating of the sample (not exceeding 80–100°C). For example, the UST was demonstrated to induce the reconstruction of defects and their complexes [9] and enhance the diffusion of defects [10] in silicon. The UST of irradiated silicon was also found to restore the conductivity [11], cause the transformation of defects [12], and recover the carrier lifetime [13], but a mechanism of these UST effects was not elucidated in detail. It was also reported that the UST influences the current–voltage characteristics of Si structures and solar cells [14, 15].

The present Letter presents the experimental data for and describes a possible mechanism of the UST-induced suppression of radiation defects and the recovery of carrier lifetime in FZ-Si. The data can find application in the development of integral detectors comprising a Si-detector and a piezoelectric substrate, which can ensure a proper UST in the course of device exploitation so as to increase its working life.

Experiments were performed on (111)-oriented volume samples of *n*-type FZ-Si with a residual boron concentration of $\sim 10^{12}$ cm^{-3} and a dopant (phosphorus) concentration within 2×10^{12}–4.5×10^{13} cm^{-3}. The samples were irradiated by γ-photons from a ^{60}Co source to a total dose of 5×10^6–2×10^7 rad and chemically polished by etching in a HNO_3–HF–CH_3COOH (3 : 1 : 1 v/v) mixture. Isochronous thermal annealing was carried out at various temperatures from 100 to 250°C as described elsewhere [16]. The distribution of microdefects was studied using the methods of surface carrier lifetime scanning [17] and selective chemical etching of defects [18]. The data presented below were mostly obtained on irradiated samples with a swirl pattern of the distribution of microdefects. The etch pits revealed the presence of

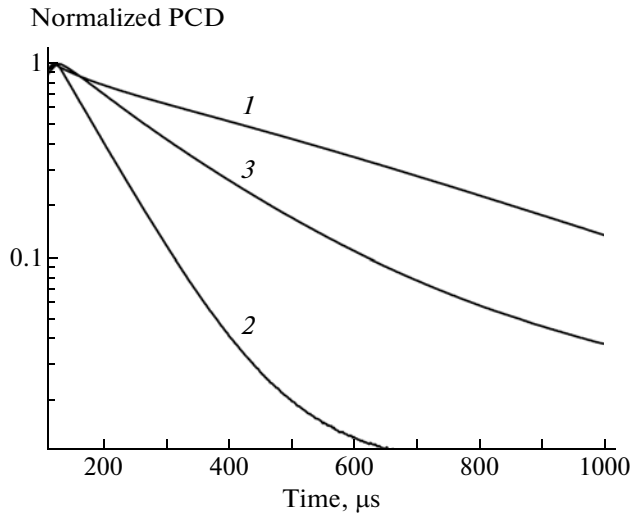

Fig. 1. Photoconductivity decay (PCD) kinetics in Si samples (*1*) before and (*2*) after γ-irradiation an (*3*) after the subsequent UST. Initial portions of the curves correspond to exponents with constant effective lifetimes τ_f.

dislocation loops (1–5 mm in diameter), which corresponded to the A-type defects.

The minority carrier lifetime was determined by the method of photoconductivity decay at a low level of injection ($\Delta\sigma/ < 0.01$) [19] on the samples with GaZn ohmic contacts. The photoconductivity was measured using 100-μs radiation pulses of a light-emitting diode (LED) operating at 1.06 μm and an interface with fast-response analog-to-digital converter. The deep-level transient spectroscopy (DLTS) measurements were performed by a standard method [20] using a Schottky barrier created by the vacuum deposition of Au onto the sample surface.

For the excitation of ultrasound, a rectangular sample (typically, 3 × 6 × 10 mm) was glued onto a piezoceramic transducer possessing a resonance frequency of 3.3 MHz. The maximum amplitude of mechanical stresses in the sample, which was numerically calculated by the finite elements method as described in [21], amounted to $\sim 10^{-4}$, which corresponded to a maximum displacement amplitude of $\sim 4 \times 10^{-8}$ m. The sample temperature was monitored using a Cu–Co thermocouple.

Figure 1 shows the typical curves of photoconductivity decay (PCD) kinetics, where the presence of a long-term component is indicative of the existence of traps. However, since the contribution of this component to the response signal amplitude is only about 2%, the recombination lifetime is reliably determined from the slope of the linear portion of PCD curves plotted on the semilogarithmic scale. This τ_f value represents an effective lifetime, which is recalculated to the bulk lifetime τ_b as described in [19].

The γ-irradiation leads to a sharp decrease in τ_b and the corresponding acceleration of PCD kinetics

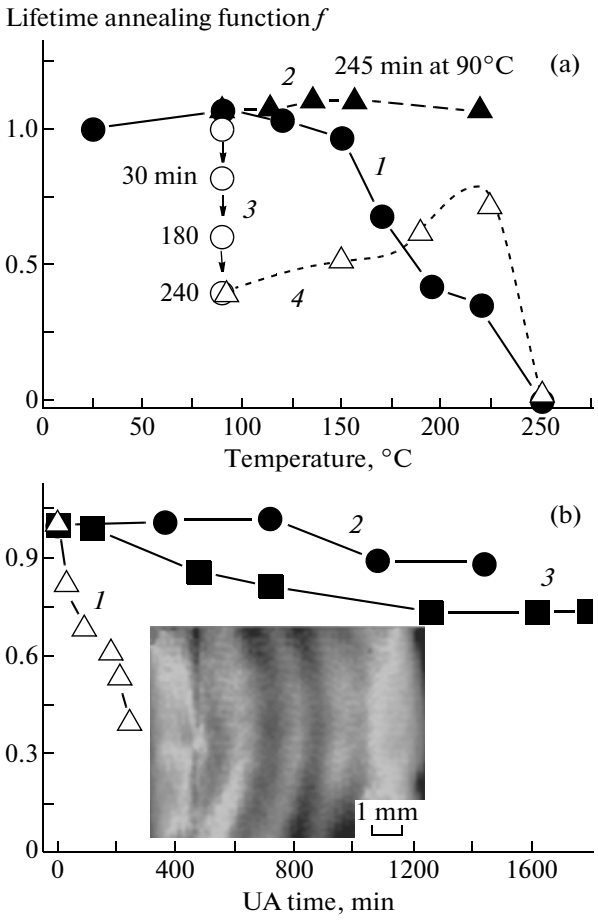

Fig. 2. Plots of (a) recovery function f (*1*) versus temperature of 15-min isochronous annealing of FZ-Si (ρ = 4 kΩ cm), (*2*) during long-term annealing at 90°C, (*3*) during ultrasonic annealing by UST for increasing times, and (*4*) versus temperature of thermal annealing after preliminary UST; (b) recovery function f versus UST time for various FZ-Si samples with (*1*) swirl pattern in the surface distribution of τ_{b0} (see inset, where the bright regions correspond to τ_{b0} increased by up to 8%) (ρ = 4 kΩ cm), (*2*) threading dislocations with a density of $\sim 10^5$ cm^{-2} (ρ = 120 Ω cm), and (*3*) perfect surface structure without swirls and dislocations (ρ = 800 Ω cm).

(Fig. 1, curve *2*). On the contrary, the subsequent UST increases the decay time (curve *3*), which is indicative of increased in τ_b and is evidence of a "cold" ultrasonic annealing of the radiation-induced defects. The recovery of τ_b can be characterized by the function $f = (\tau_{ba}^{-1} - \tau_{b0}^{-1})/(\tau_{birr}^{-1} - \tau_{b0}^{-1})$, where τ_{b0} and τ_{birr} are the carrier lifetimes before and after γ-irradiation, respectively, and τ_{ba} is that after the UST (or thermal annealing) as determined from curves *1–3* in Fig. 1. Comparative data for the ultrasonic and thermal treatments of γ-irradiated Si samples are presented in Fig. 2.

The observed character of thermal annealing can be explained as related to the contribution from at least two types of defects, which are annealed at $T \approx$

150 and 225°C (Fig. 2a, curve *1*). The first stage of τ_b recovery at ~150°C is consistent with the annealing of *E*-type centers [representing vacancy–phosphorus atom (*V–P*) complexes], while the subsequent stage at ~225°C can be related to the annealing of divacancies (V_2) [22].

It should be noted that the ultrasonic annealing takes place at a relatively low temperature of the sample (~90°C), which is determined by the intensity of ultrasound, and a decrease in *f* depends on the UST duration (Fig. 2a, curve *3*). On the contrary, attempts at prolonged thermal annealing at 90°C did not lead to any significant change in *f* (Fig. 2a, curve *3*). It should be emphasized that isochronous heat treatment of a sample upon the ultrasonic annealing treatment reveals additional features—in particular, an increase in *f* in the region of ~150–225°C (Fig. 2a, curve *4*), which indicate that the ultrasonic annealing is not a purely thermal process.

The ultrasonic annealing is most pronounced in FZ-Si samples with a swirl pattern of defects (Fig. 2b, curve *1*). In cases where the formation of a swirl structure of microdefects is suppressed by dislocations, the UST effect is much less pronounced (curve *2*). The samples with minimum concentrations of extended defects exhibit an intermediate level of ultrasonic annealing (curve *3*). Therefore, it can be suggested that microdefects act as sinks for the defects released under the action of ultrasound, with a maximum effect for the swirl pattern of defects (curve *1*).

It was previously established [9, 21] that UST could probably induce an over-barrier displacement of defects. Therefore, by analogy with the case of thermal annealing, the disappearance of E-type centers during the UST can be determined by two processes, including (i) the dissociation of *V–P* complexes in the field of mechanical stresses and (ii) the diffusion of released vacancies to sinks. However, in contrast to the thermal annealing, the UST is accompanied by a significant growth in the concentration of V_2, which is confirmed by the increase in *f* in a temperature interval of the thermal annealing of V_2 (Fig. 2a, curve *4*).

Taking into account the standing character of ultrasonic waves, it can be suggested that vacancies are released from *V–P* complexes only in the regions of strain antinodes and then pushed toward the strain nodes. As a result, the degree of τ_b recovery relative to the irradiation-deteriorated level did not exceed 70% ($f \approx 0.3$ for curve *3* in Fig. 2a). In the vicinity of a microdefect, a vacancy is trapped by electrically inactive complexes. The subsequent thermal annealing converts vacancies into active complexes (V_2), which account for the growth of *f* on curve *4* (Fig. 2a).

Figure 3 shows the Arrhenius plots of DLTS peak intensity in various Si samples studied. The γ-irradiated sample exhibits a level with $E = 0.37 \pm 0.02$ eV (curve *1*, Fig. 3), which corresponds to a E-type center [23]. A combination of the UST with subsequent thermal treatment reveals a level with $E = 0.18 \pm 0.01$ eV (curve *2*, Fig. 3), which can be attributed to a V–O complex (A-type center) [23]. This fact can be explained by assuming that V_2 complexes formed in the vicinity of microdefects are decomposed by thermal treatment and the released vacancies are trapped by oxygen atoms (present in the atmosphere of these defects) with the formation of more thermally stable A-type centers. These V–O complexes do not affect the recombination of nonequilibrium carriers, since the Fermi level is much below the level of A-type centers. In the sample that was only thermally annealed after the γ-irradiation, the DLTS data reveal a level at $E = 0.09 \pm 0.01$ eV (curve *3*, Fig. 3), which has been previously observed in irradiated FZ-Si [24] but yet not reliably identified. In particular, this was related to thermal donors in silicon [25], which could also be present in the samples under consideration.

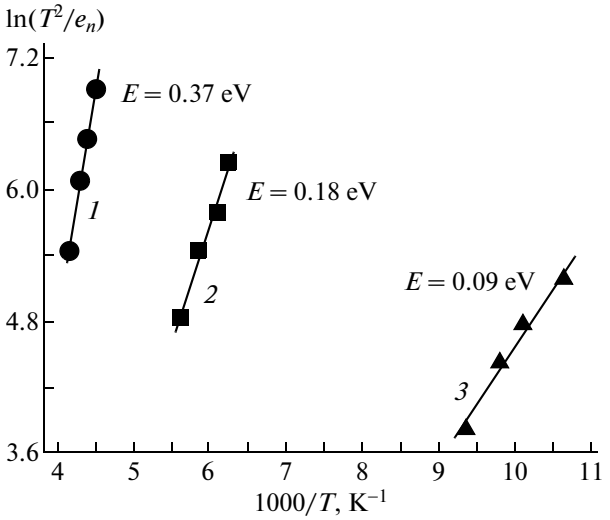

Fig. 3. Plots of T_2-corrected coefficients of thermal emission for the centers of three types revealed by DLTS in Si samples (with energies *E* determined from the slopes of curves *1–3*).

Thus, the UST-induced recovery of the carrier recombination lifetime in irradiation-damaged Si may be related to the release of vacancies from E-type centers and their subsequent trapping on sinks. This treatment opens ways to increasing the working life of Si-detectors and related devices employed under elevated irradiation levels.

Acknowledgments. The authors are grateful to V.I. Khivrich (Kiev Institute for Nuclear Research, National Academy of Sciences of Ukraine, Kiev) for his help in conducting irradiation of silicon samples.

REFERENCES

1. M. Bruzzi, IEEE Trans. Nucl. Sci. **48** (4), 960 (2001).
2. Y. Yamamoto, O. Kawasaki, S. Matsuda, and Y. Morita, *Proceedings of the European Space Power Conference*

(September 4–8, 1995, Poitiers, France), ESA SP-369 (1995), pp. 573–578.
3. G. Lindstrum, M. Moll, and E. Fretwurst, Nucl. Instrum. Meth. Phys. Res. A **426** (1), 1 (1999).
4. http://rd50.web.cern.ch/rd50/.
5. H. F.-W. Sadrozinski, IEEE Trans. Nucl. Sci. **48** (4), 933 (2001).
6. M. Bruzzi, D. Bisello, L. Borrello, E. Borchi, et al., Nucl. Instrum. Meth. Phys. Res. A **552** (1-2), 20 (2005).
7. T. Maekava, S. Inoue, A. Aiura, and A. Usami, Semicond. Sci. Technol. **1** (5), 305 (1986).
8. C. A. Londos, M. S. Potsidi, A. Misiuk, J. Ratajczak, V. V. Emtsev, and G. Antonaras, J. Appl. Phys. **94** (7), 4363 (2003).
9. S. Ostapenko, N. E. Korsunskaya, and M. K. Sheinkman, Solid State Phenom. **85–86**, 317 (2002).
10. V. D. Krevchik, R. A. Muminov, and A. Ya. Yafasov, Phys. Status Solidi (a) **63** (2), K159 (1981).
11. I. V. Ostrovskii and O. A. Korotchenkov, Sov. Phys. Tech. Phys. **31**, 11 (1986).
12. Ya. M. Olikh, N. D. Timochko, and A. P. Dolgolenko, Tech. Phys. Lett. **32**, 586 (2006).
13. A. A. Podolyan and V. I. Khivrich, Tech. Phys. Lett. **31**, 408 (2005).
14. A. Guseynov, Ya. M. Olikh, and Sh. G. Askerov, Tech. Phys. Lett. **33**, 18 (2007).
15. A. M. Gorb, O. Ya. Olikh, A. O. Podolian, and O. A. Korotchenkov, IEEE Trans. Nucl. Sci. **57** (3), 1632 (2010).
16. A. K. Semenyuk, V. I. Khivrich, and I. D. Konozenko, Phys. Status Solidi (a) **7** (1), 51 (1971).
17. A. Podolian, A. Nadtochiy, V. Kuryliuk, O. Korotchenkov, J. Schmid, M. Drapalik, and V. Schlosser, Solar Energy Mater. Solar Cells **95** (2), 765 (2011).
18. F. Secco D'aragona, Phys. Status Solidi (a) **7** (2), 577 (1971).
19. D. K. Schroder, *Semiconductor Material and Device Characterization*, 2nd ed. (Wiley-Interscience, New York, 1998).
20. S. Misrachi, A. R. Peaker, and B. Hamilton, J. Phys. E: Sci. Instrum. **13** (10), 1055 (1980).
21. A. Podolian, V. Kuryliuk, and O. Korotchenko, Solar Energy Mater. Solar Cells **93** (11), 1946 (2009).
22. H. J. Stein, in *Radiation Effects in Semiconductors*, Ed. by J. W. Corbett and G. D. Watkins (Gordon and Breach, New York, 1971), p. 125.
23. F. D. Auret and P. N. K. Deenapanray, Crit. Rev. Solid State Mater. Sci. **29** (1), 1 (2004).
24. S. D. Brotheron and J. Bradley, Appl. Phys. **53** (8), 5720 (1982).

Translated by P. Pozdeev